



Ethyl 5-methyl-3-[11-(pyridin-2-yl)-6,11-dihydro-6,11-epoxydibenzo[*b,e*]oxepin-6-yl]isoxazole-4-carboxylate: a bicyclic acetal from the rearrangement of an anthracenyl isoxazole

Matthew J. Weaver,^{a‡} Michael J. Campbell,^a Chun Li^b and Nicholas R. Natale^{a*}

Received 20 October 2020

Accepted 28 October 2020

Edited by W. T. A. Harrison, University of Aberdeen, Scotland

‡ Current address: Elite One Source, Nutritional Services, 1001 South 3rd West, Missoula, MT 59801 USA.

Keywords: crystal structure; epoxy-dibenzo[*b,e*]oxepin; isoxazole; anthracenyl isoxazole.

CCDC reference: 2041149

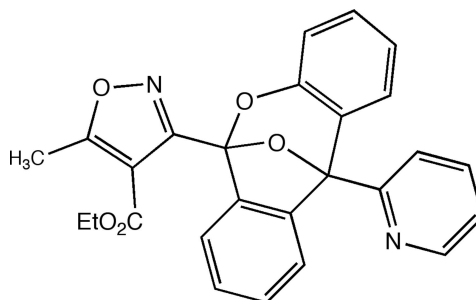
Supporting information: this article has supporting information at journals.iucr.org/e

^aDepartment of Biomedical & Pharmaceutical Sciences, University of Montana, Missoula, MT 59812, USA, and ^bDepartment of Chemistry, Ithaca College, 953 Danby Road, Ithaca, NY 14850, USA. *Correspondence e-mail: nicholas.natale@mso.umt.edu

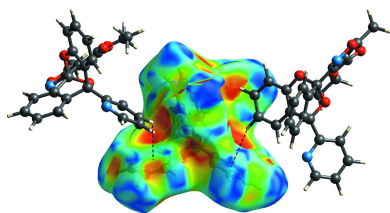
The title compound, C₂₆H₂₀N₂O₅, is a rearrangement product of an *o*-pyridinyl anthracenyl isoxazole ester. It features a bicyclic acetal structure, which has two extended almost co-planar ring systems, which subtend a fold angle of 102.17 (5)°. In the crystal, the molecules are closely knitted together through C—H···N and C—H···O hydrogen bonds and form chains of alternating enantiomers propagating along the *c*-axis direction.

1. Chemical context

We have reported on 3-aryl isoxazole amides (AIMs) with antitumor activity (Han *et al.*, 2009; Weaver *et al.*, 2015) and recently described 10-substituted anthracenes with N-heterocyclic substituents in this series, which possessed robust antitumor activity against both breast and brain tumor cell lines (Weaver *et al.*, 2020). In the course of that study, we attempted to obtain crystals of the 10-*o*-pyridyl example **II** by slow evaporation (see Fig. 1). After numerous attempts, suitable crystals were obtained but were found to have undergone oxygen addition and rearrangement to the title compound, C₂₆H₂₀N₂O₅, **I**. This is unprecedented in this series of compounds.



In the case of the *o*-pyridyl ester, slow evaporation from solution was observed to produce a bicyclic acetal (BA). This requires the formation of a dioxygen adduct commonly found in the anthracene literature (Klaper *et al.*, 2016), as shown in Fig. 1. This dioxygen adduct **III** is most often observed as a [4 + 2] cycloadduct with singlet oxygen (Lauer *et al.*, 2011), and in some cases where a donor–acceptor pair sensitizes the formation of singlet oxygen. It should be noted, however, that the endo peroxide can be formed from the ground-state diradical oxygen in a one-electron process.



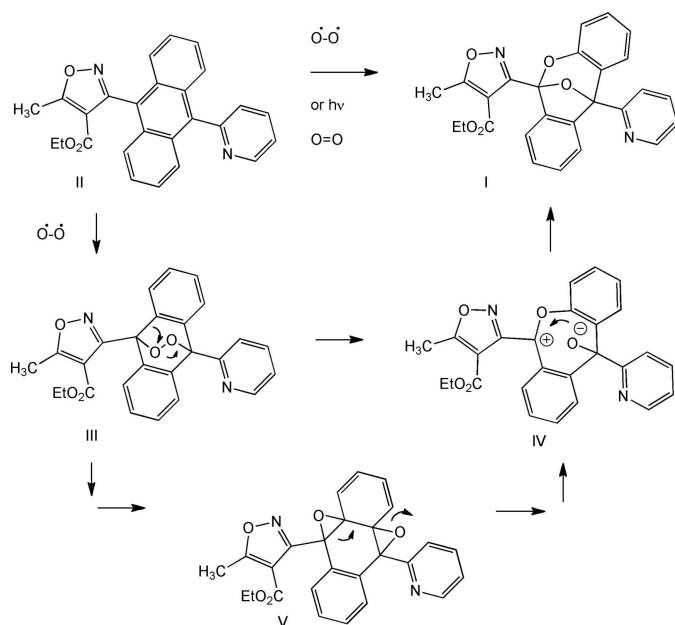


Figure 1
Rearrangement of *o*-pyridyl ester **II**. The title compound **I** was observed on slow evaporation during recrystallization at room temperature.

The bicyclic acetal (BA) **I** can be formed directly *via* a Criegee-like rearrangement through intermediate **IV**, or alternatively stepwise *via* the intermediacy of one electron reorganization to an intermediate diepoxide **V** (Filatov *et al.*, 2017). Of the ten previous crystal structures of anthryl isoxazoles published by our group (Mosher *et al.*, 1996; Han *et al.*, 2002, 2003; Li *et al.*, 2006, 2008; Li *et al.*, 2013; Duncan *et al.*, 2014; Weaver *et al.*, 2015), and the three N-heterocyclic structures solved and disclosed (Weaver *et al.*, 2020), this is the first example we have observed of this rearrangement. Given the observation of this rearrangement it is advisable that the *o*-pyridyl AIM (**III**) be stored under an argon atmosphere at low temperature (233 K or below).

Conditions within tumors are notoriously anoxic. As an example, the transition to the Warberg phenotype (Vander Heiden *et al.*, 2009) is heavily influenced by the transcription factor hypoxia inducing factor (HIF). Therefore, the physiological relevance and therapeutic practicality of this process appears questionable, particularly considering that the *endo* peroxide (**III**) or the diepoxide (**V**) would not be expected to exert significant selectivity. Therefore, the probability of a useful therapeutic index would appear low. However, the prospects for exploiting this tactic will be considered, even if they constitute only negative controls, in our ongoing studies of antitumor theranostics, and will be reported in due course.

2. Structural commentary

The title compound crystallizes as a racemate in the monoclinic space group, $P2_1/c$, with one independent molecule in the asymmetric unit (Fig. 2). In the arbitrarily chosen asymmetric molecule, atoms C7 and C14 both have *R* configura-

tions. The insertion of two oxygen atoms in the central ring of anthracene forms a bicyclic system with one oxygen atom (O1) in the middle shared by both dioxane and furan rings. The remainder of the dioxane and furan ring atoms are co-planar with the C1–C6 and C8–C13 benzene rings on either side, respectively. The pyridine group is attached at the *ortho* position to one of the shared carbon atoms on the bicyclic system, while the isoxazole ester is attached to the other shared carbon atom. The overall effect of the bonding gives the whole molecule a dragon-like appearance.

The planarity of each wing is indicated by the r.m.s.d. of 0.028 Å for both planes formed by C1–C7/C14/O2 and C7–C14. These two wings are flapping downwards with a fold angle between them of 102.17 (5)°. The pyridine group is the head of the dragon with the nitrogen atom being *exo* to the oxygen atom (O1) in the backbone. A potential hydrogen bond between C23–H23 and O1 may contribute to the small torsion angle of 2.2 (3)° for O1–C7–C22–C23. Both the nitrogen and oxygen atoms in the isoxazole ring are *exo* to the oxygen atoms (O1 and O2) in the dioxane ring, resulting in the ethyl ester tail swinging to the dioxane side and coming to rest between the two oxygen atoms. There is a σ – π interaction between the tip of the tail (methyl group) and the benzene ring, which is also reflected by the upfield shift of CH₃ protons in the NMR spectrum.

3. Supramolecular features

In the crystal, chains of alternating enantiomers are formed running along the *c*-axis direction through the intermolecular hydrogen bonds C23–H23⋯N1ⁱ, C12–H12⋯O1ⁱⁱ and C18–H18B⋯O4ⁱⁱ (Table 1, Fig. 3). This chain is highly

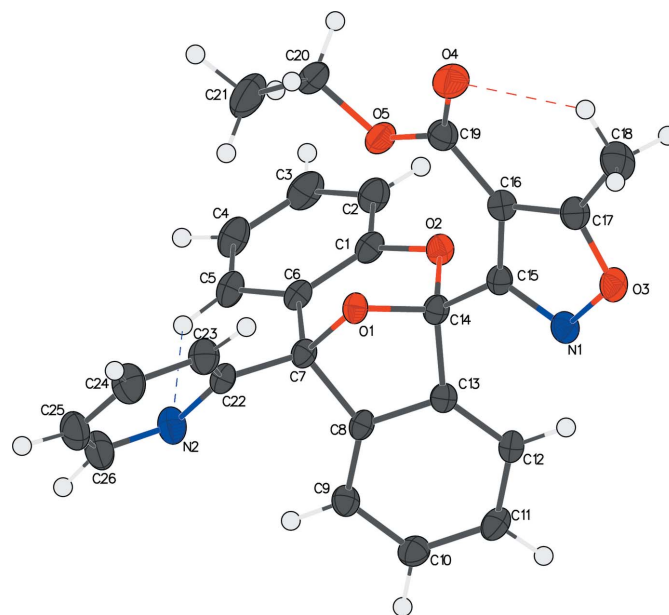


Figure 2
The molecular structure of **I** showing the atom-labeling scheme. Displacement ellipsoids are drawn at the 50% probability level. Dashed lines indicate intramolecular hydrogen bonds.

Table 1
 Hydrogen-bond geometry (Å, °).

$D-H\cdots A$	$D-H$	$H\cdots A$	$D\cdots A$	$D-H\cdots A$
C5—H5 \cdots N2	0.96 (2)	2.42 (2)	3.085 (3)	125.8 (18)
C23—H23 \cdots N1 ⁱ	1.00 (3)	2.70 (3)	3.669 (3)	163 (2)
C12—H12 \cdots O1 ⁱⁱ	0.94 (3)	2.56 (3)	3.469 (2)	162 (2)
C18—H18A \cdots O4 ⁱⁱ	0.94 (4)	2.71 (4)	3.297 (3)	121 (3)
C18—H18B \cdots O4	0.99 (4)	2.38 (4)	3.040 (3)	123 (3)

 Symmetry codes: (i) $x, -y + \frac{1}{2}, z - \frac{1}{2}$; (ii) $x, -y + \frac{1}{2}, z + \frac{1}{2}$.

knitted, which may contribute to the formation of needle-shaped crystals.

4. Hirshfeld surface analysis

The intermolecular interactions were quantified using Hirshfeld surface analysis (Spackman & Jayatilaka, 2009) and the associated two-dimensional fingerprint plots (McKinnon *et al.*, 2007). The calculations and visualization were performed using *CrystalExplorer17* (Turner *et al.*, 2017). The Hirshfeld surface of the title compound is mapped over d_{norm} in a fixed color scale of -0.1374 (red) to $+1.3125$ (blue) arbitrary units (Fig. 4), where the red spots indicate the intermolecular contacts shorter than the van der Waals separations. The delineated two-dimensional fingerprint plots are shown in Fig. 5, and demonstrate that the main contribution to the overall Hirshfeld surface area arises from $H\cdots H$ contacts (50.5%, Fig. 5a). The $C\cdots H/H\cdots C$ contacts (24.7%, Fig. 5b), which indicate $C-H\cdots\pi$ interactions, are identifiable from

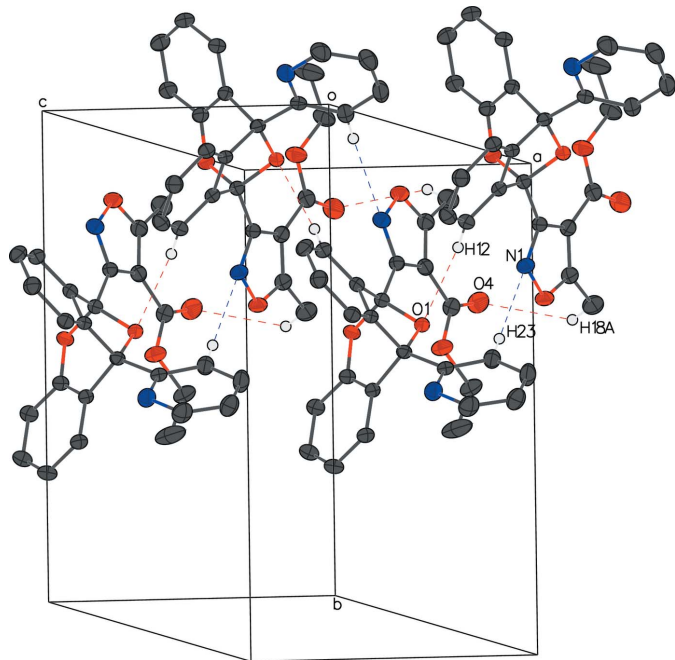


Figure 3
 The packing of **I**. A closely knitted chain of alternating enantiomers is formed through several intermolecular hydrogen bonds. For clarity, H atoms not participating in intermolecular bonds are omitted. Atoms participating in intermolecular hydrogen bonds are labeled once.

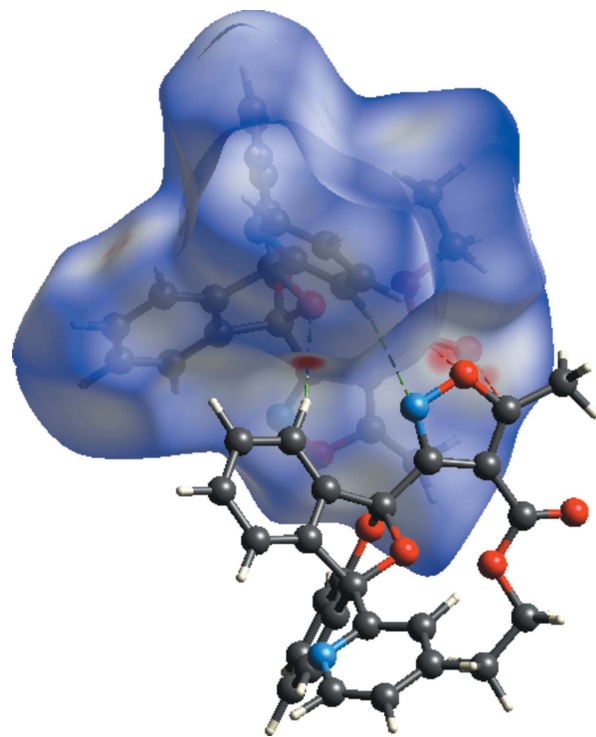


Figure 4
 Hirshfeld surface of **I** mapped over d_{norm} . Short contacts between carbonyl C19=O3 and isoxazole O3—C17 are shown in dashed red lines. Intermolecular hydrogen bonds O1 \cdots H12 and N1 \cdots H23 are shown as dashed green lines.

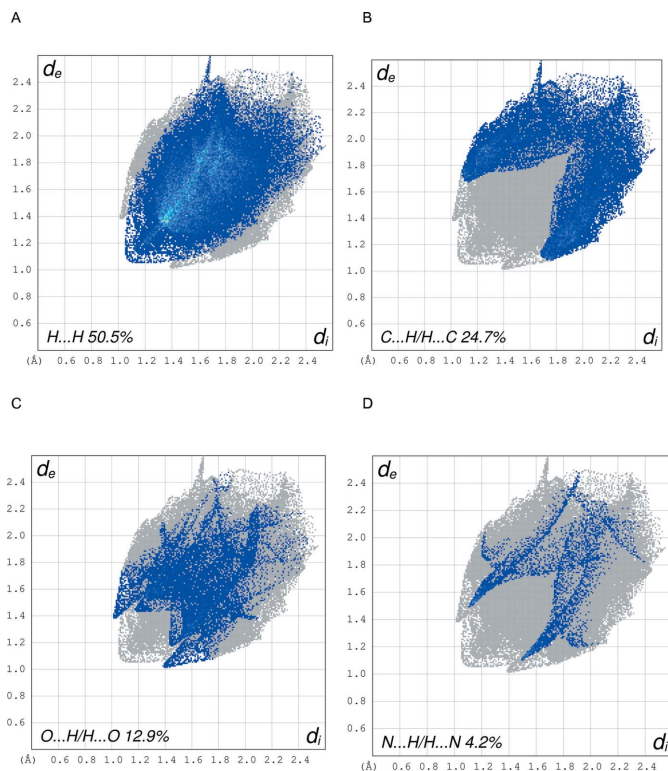


Figure 5
 The two-dimensional fingerprint plots for **I** delineated into (a) $H\cdots H/H\cdots H$ contacts, (b) $C\cdots H/H\cdots C$ contacts, (c) $O\cdots H/H\cdots O$ contacts, and (d) $N\cdots H/H\cdots N$ contacts.

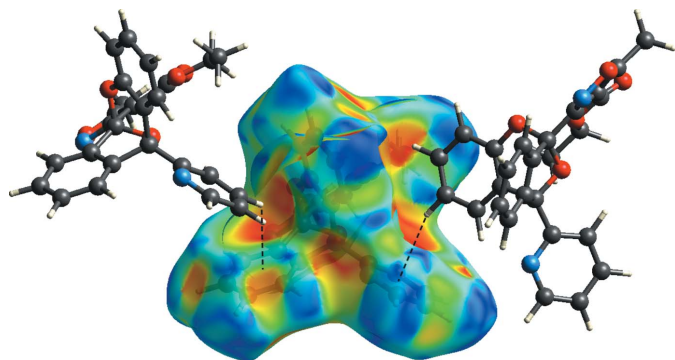


Figure 6

Hirshfeld surface of **I** mapped over the shape-index property. C—H... π interactions (C24—H24 to aromatic ring C1—C6 and C4—H4 to aromatic ring N22/C22—C26) are shown as dashed lines.

the Hirshfeld surface mapped over the shape-index property (Fig. 6). Conventional hydrogen-bonding interactions, H...O/O...H and N...H/H...N, only comprise 12.9% and 4.2% of the intermolecular interactions, respectively (Fig. 5b and 5c).

5. Database survey

A search for the 6,11-dihydro-6,11-epoxydibenzo[*b,e*]oxepin fragment in the Cambridge Structural Database (CSD version 5.40, August 2019 update; Groom *et al.*, 2016) resulted in five hits, namely refcodes LIPZEP (Walker *et al.*, 1999), NEJLOG (Filatov *et al.*, 2017), VAZDEI, VAZDIM (Ando *et al.*, 2017), and WOPGAM (Ando *et al.*, 2019). These five structures, despite their different substitution groups and positions, all exhibit a similar structural configuration, that with shared oxygen atom pointing up, and the remainder of the five- and seven-membered rings on the bicyclic system are co-planar to their respective benzene rings.

6. Synthesis and crystallization

The title compound was synthesized from the *o*-pyridyl-anthracenyl isoxazole ester (**II**) (Weaver *et al.*, 2020). Colorless needles were obtained by slow evaporation in the presence of atmospheric oxygen over a period of several months. ¹H NMR (CDCl₃) δ ppm 8.895 (*d*, 1H, *J* = 5 Hz); 8.13 (*dd*, 1H, *J* = 6 Hz); 7.8 (*d*, 2H, *J* = 4 Hz); 7.57 (*dt*, 1H); 7.34 (*m*, 4H); 7.16 (*m*, 1H); 6.85 (*d*, 1H, 8 Hz); 6.79 (*t*, 1H, *J* = 8 Hz); 3.975 (*q*, 1H, *J* = 7 Hz); 3.845 (*q*, 1H, *J* = 7 Hz); 2.79 (*s*, 3H); 0.63 (*t*, 3H, *J* = 7 Hz). ¹³C NMR (CDCl₃) δ ppm 176.69, 161.73 158.05, 156.86, 150.24, 148.55, 146.15, 135.98, 136.88, 129.35, 128.44, 128.17, 123.27, 123.09, 122.16, 121.46, 121.35, 120.46, 117.01, 60.91, 13.14. 13.08. The proton–proton correlation is provided in the supporting information. Positive electrospray ionization (ESI) mass spectrometry, calc. for [C₂₆H₂₀N₂O₃+H]⁺ 441.44, observed *m/z* 441.2 ([*M* + H]⁺, 100% rel. intensity).

Table 2

Experimental details.

Crystal data	
Chemical formula	C ₂₆ H ₂₀ N ₂ O ₃
<i>M_r</i>	440.44
Crystal system, space group	Monoclinic, <i>P</i> 2 ₁ / <i>c</i>
Temperature (K)	150
<i>a</i> , <i>b</i> , <i>c</i> (Å)	19.0586 (7), 13.9627 (5), 8.1459 (3)
β (°)	101.7800 (11)
<i>V</i> (Å ³)	2122.05 (13)
<i>Z</i>	4
Radiation type	Synchrotron, λ = 0.7288 Å
μ (mm ⁻¹)	0.10
Crystal size (mm)	0.11 × 0.01 × 0.01
Data collection	
Diffractometer	Bruker PHOTON-II
Absorption correction	Multi-scan (<i>SADABS</i> ; Krause <i>et al.</i> , 2015)
No. of measured, independent and observed [<i>I</i> > 2 σ (<i>I</i>)] reflections	71254, 5275, 3947
<i>R</i> _{int}	0.067
(<i>sin</i> θ / λ) _{max} (Å ⁻¹)	0.667
Refinement	
<i>R</i> [<i>F</i> ² > 2 σ (<i>F</i> ²)], <i>wR</i> (<i>F</i> ²), <i>S</i>	0.052, 0.145, 1.05
No. of reflections	5275
No. of parameters	378
H-atom treatment	All H-atom parameters refined
$\Delta\rho_{\text{max}}$, $\Delta\rho_{\text{min}}$ (e Å ⁻³)	0.28, -0.27

Computer programs: *APEX3* and *SAINT* (Bruker, 2016), *SHELXS* (Sheldrick, 2008), *SHELXL* (Sheldrick, 2015), *OLEX2* (Dolomanov *et al.*, 2009), and *pubCIF* (Westrip, 2010).

7. Refinement

Crystal data, data collection and structure refinement details are summarized in Table 2. All hydrogen atoms were found in difference-Fourier maps and their positions were freely refined with the constraint $U_{\text{iso}}(\text{H}) = 1.2$ or $1.5U_{\text{eq}}(\text{parent})$. Seven reflections were omitted because of poor agreement between the observed and calculated intensities.

Acknowledgements

The authors thank the ALSAM Foundation for support of this work. The authors thank Dr Allen G. Oliver (University of Notre Dame) and Dr Jeanette A. Krause (University of Cincinnati) for the synchrotron data collected through the SCrALS (Service Crystallography at the Advanced Light Source) program at Beamline 12.2.1, Advanced Light Source (ALS), Lawrence Berkeley National Laboratory. The Advanced Light Source, is a DOE Office of Science User Facility under contract No. DE-AC02-05CH11231. CL is grateful for both Dr Krause's guidance in processing synchrotron data and her helpful comments that improved the manuscript.

Funding information

Funding for this research was provided by: ALSAM Foundation Skaggs Scholar Grant (grant No. #1000233768 to Nicholas R. Natale); University of Montana (grant No. 325490 to Nicholas R. Natale).

References

- Ando, Y., Hanaki, A., Sasaki, R., Ohmori, K. & Suzuki, K. (2017). *Angew. Chem. Int. Ed.* **56**, 11460–11465.
- Ando, Y., Tanaka, D., Sasaki, R., Ohmori, K. & Suzuki, K. (2019). *Angew. Chem. Int. Ed.* **58**, 12507–12513.
- Bruker (2016). *SAINT* and *APEX3*. Bruker AXS Inc., Madison, Wisconsin, USA.
- Dolomanov, O. V., Bourhis, L. J., Gildea, R. J., Howard, J. A. K. & Puschmann, H. (2009). *J. Appl. Cryst.* **42**, 339–341.
- Duncan, N. S., Beall, H. D., Kearns, A. K., Li, C. & Natale, N. R. (2014). *Acta Cryst.* **E70**, o315–o316.
- Filatov, M. A., Karuthedath, S., Polestshuk, P. M., Savoie, H., Flanagan, K. J., Sy, C., Sitte, E., Telitchko, M., Laquai, F., Boyle, R. W. & Senge, M. O. (2017). *J. Am. Chem. Soc.* **139**, 6282–6285.
- Groom, C. R., Bruno, I. J., Lightfoot, M. P. & Ward, S. C. (2016). *Acta Cryst.* **B72**, 171–179.
- Han, X., Li, C., Mosher, M. D., Rider, K. C., Zhou, P., Crawford, R. L., Fusco, W., Paszczyński, A. & Natale, N. R. (2009). *Bioorg. Med. Chem.* **17**, 1671–1680.
- Han, X., Li, C., Rider, K. C., Blumenfeld, A., Twamley, B. & Natale, N. R. (2002). *Tetrahedron Lett.* **43**, 7673–7677.
- Han, X., Twamley, B. & Natale, N. R. (2003). *J. Heterocycl. Chem.* **40**, 539–545.
- Klaper, M., Wessig, P. & Linker, T. (2016). *Chem. Commun.* **52**, 1210–1213.
- Krause, L., Herbst-Irmer, R., Sheldrick, G. M. & Stalke, D. (2015). *J. Appl. Cryst.* **48**, 3–10.
- Lauer, A., Dobryakov, A. L., Kovalenko, S. A., Fidler, H. & Heyne, K. (2011). *Phys. Chem. Chem. Phys.* **13**, 8723–8732.
- Li, C., Campbell, M. J., Weaver, M. J., Duncan, N. S., Hunting, J. L. & Natale, N. R. (2013). *Acta Cryst.* **E69**, o1804–o1805.
- Li, C., Twamley, B. & Natale, N. R. (2006). *Acta Cryst.* **E62**, o854–o856.
- Li, C., Twamley, B. & Natale, N. R. (2008). *J. Heterocycl. Chem.* **45**, 259–264.
- McKinnon, J. J., Jayatilaka, D. & Spackman, M. A. (2007). *Chem. Commun.* pp. 3814–3816.
- Mosher, M. D., Natale, N. R. & Vij, A. (1996). *Acta Cryst.* **C52**, 2513–2515.
- Sheldrick, G. M. (2008). *Acta Cryst.* **A64**, 112–122.
- Sheldrick, G. M. (2015). *Acta Cryst.* **C71**, 3–8.
- Spackman, M. A. & Jayatilaka, D. (2009). *CrystEngComm.* **11**, 19–32.
- Turner, M. J., McKinnon, J. J., Wolff, S. K., Grimwood, D. J., Spackman, P. R., Jayatilaka, D. & Spackman, M. A. (2017). *CrystalExplorer17*. University of Western Australia. <http://hirshfeldsurface.net>
- Vander Heiden, M. G., Cantley, L. C. & Thompson, C. B. (2009). *Science*, **324**, 1029–1033.
- Walker, M., Pohl, E., Herbst-Irmer, R., Gerlitz, M., Rohr, J. & Sheldrick, G. M. (1999). *Acta Cryst.* **B55**, 607–616.
- Weaver, M. J., Kearns, A. K., Stump, S., Li, C., Gajewski, M. P., Rider, K. C., Backos, D. S., Reigan, P. R., Beall, H. D. & Natale, N. R. (2015). *Bioorg. Med. Chem. Lett.* **25**, 1765–1770.
- Weaver, M. J., Stump, S., Campbell, M. J., Backos, D. S., Li, C., Reigan, P., Adams, E., Beall, H. D. & Natale, N. R. (2020). *Bioorg. Med. Chem.* **28**, 115781.
- Westrip, S. P. (2010). *J. Appl. Cryst.* **43**, 920–925.

supporting information

Acta Cryst. (2020). E76, 1818-1822 [https://doi.org/10.1107/S2056989020014358]

Ethyl 5-methyl-3-[11-(pyridin-2-yl)-6,11-dihydro-6,11-epoxy-dibenzo[*b,e*]oxepin-6-yl]isoxazole-4-carboxylate: a bicyclic acetal from the rearrangement of an anthracenyl isoxazole

Matthew J. Weaver, Michael J. Campbell, Chun Li and Nicholas R. Natale

Computing details

Data collection: *APEX3* (Bruker, 2016); cell refinement: *SAINTE* (Bruker, 2016); data reduction: *SAINTE* (Bruker, 2016); program(s) used to solve structure: *SHELXS* (Sheldrick, 2008); program(s) used to refine structure: *SHELXL* (Sheldrick, 2015); molecular graphics: *OLEX2* (Dolomanov *et al.*, 2009); software used to prepare material for publication: *publCIF* (Westrip, 2010).

Ethyl 5-methyl-3-[11-(pyridin-2-yl)-6,11-dihydro-6,11-epoxydibenzo[*b,e*]oxepin-6-yl]isoxazole-4-carboxylate

Crystal data

C₂₆H₂₀N₂O₅

M_r = 440.44

Monoclinic, *P2₁/c*

a = 19.0586 (7) Å

b = 13.9627 (5) Å

c = 8.1459 (3) Å

β = 101.7800 (11)°

V = 2122.05 (13) Å³

Z = 4

F(000) = 920

D_x = 1.379 Mg m⁻³

Synchrotron radiation, λ = 0.7288 Å

Cell parameters from 9997 reflections

θ = 2.7–29.0°

μ = 0.10 mm⁻¹

T = 150 K

Needle, colourless

0.11 × 0.01 × 0.01 mm

Data collection

Bruker PHOTON-II
diffractometer

Radiation source: synchrotron

Si-<111> channel cut crystal monochromator

ω–φ scans

Absorption correction: multi-scan
(SADABS; Krause *et al.*, 2015)

71254 measured reflections

5275 independent reflections

3947 reflections with *I* > 2σ(*I*)

R_{int} = 0.067

θ_{max} = 29.1°, θ_{min} = 1.1°

h = –25→25

k = –18→18

l = –10→10

Refinement

Refinement on *F*²

Least-squares matrix: full

R[*F*² > 2σ(*F*²)] = 0.052

wR(*F*²) = 0.145

S = 1.05

5275 reflections

378 parameters

0 restraints

Primary atom site location: structure-invariant
direct methods

Hydrogen site location: difference Fourier map

All H-atom parameters refined

w = 1/[σ²(*F_o*²) + (0.0476*P*)² + 2.6861*P*]

where *P* = (*F_o*² + 2*F_c*²)/3

$$(\Delta/\sigma)_{\max} < 0.001$$

$$\Delta\rho_{\max} = 0.28 \text{ e } \text{\AA}^{-3}$$

$$\Delta\rho_{\min} = -0.27 \text{ e } \text{\AA}^{-3}$$

Special details

Geometry. All esds (except the esd in the dihedral angle between two l.s. planes) are estimated using the full covariance matrix. The cell esds are taken into account individually in the estimation of esds in distances, angles and torsion angles; correlations between esds in cell parameters are only used when they are defined by crystal symmetry. An approximate (isotropic) treatment of cell esds is used for estimating esds involving l.s. planes.

Fractional atomic coordinates and isotropic or equivalent isotropic displacement parameters (\AA^2)

	<i>x</i>	<i>y</i>	<i>z</i>	$U_{\text{iso}}^*/U_{\text{eq}}$
O1	0.24461 (7)	0.07865 (10)	0.35674 (16)	0.0202 (3)
O2	0.29900 (8)	0.07367 (10)	0.64004 (17)	0.0223 (3)
O3	0.34820 (8)	0.35999 (10)	0.50102 (19)	0.0261 (3)
O4	0.47276 (9)	0.15114 (12)	0.3200 (2)	0.0361 (4)
O5	0.39223 (8)	0.05030 (11)	0.3916 (2)	0.0296 (4)
N1	0.29207 (9)	0.29999 (12)	0.5258 (2)	0.0238 (4)
N2	0.09144 (10)	-0.07696 (14)	0.2123 (2)	0.0292 (4)
C1	0.27403 (12)	-0.01948 (14)	0.6403 (3)	0.0232 (4)
C2	0.30636 (13)	-0.07614 (16)	0.7747 (3)	0.0287 (5)
C3	0.28365 (14)	-0.17036 (16)	0.7839 (3)	0.0344 (5)
C4	0.22965 (14)	-0.20738 (16)	0.6600 (3)	0.0326 (5)
C5	0.19750 (13)	-0.14975 (15)	0.5254 (3)	0.0266 (5)
C6	0.21931 (11)	-0.05535 (14)	0.5141 (2)	0.0211 (4)
C7	0.18559 (10)	0.01676 (13)	0.3788 (2)	0.0193 (4)
C8	0.14033 (11)	0.08444 (13)	0.4614 (2)	0.0193 (4)
C9	0.06981 (11)	0.07996 (15)	0.4768 (3)	0.0228 (4)
C10	0.04475 (12)	0.15003 (16)	0.5736 (3)	0.0263 (4)
C11	0.09066 (12)	0.22102 (16)	0.6540 (3)	0.0272 (5)
C12	0.16221 (11)	0.22441 (15)	0.6391 (2)	0.0226 (4)
C13	0.18632 (11)	0.15600 (14)	0.5409 (2)	0.0197 (4)
C14	0.26003 (11)	0.13279 (14)	0.5063 (2)	0.0201 (4)
C15	0.31029 (11)	0.21370 (14)	0.4879 (2)	0.0202 (4)
C16	0.37804 (11)	0.21339 (15)	0.4366 (2)	0.0227 (4)
C17	0.39812 (12)	0.30763 (15)	0.4467 (3)	0.0249 (4)
C18	0.46053 (15)	0.3608 (2)	0.4110 (4)	0.0355 (5)
C19	0.41961 (11)	0.13631 (16)	0.3764 (3)	0.0254 (4)
C20	0.42398 (14)	-0.02839 (17)	0.3144 (3)	0.0330 (5)
C21	0.38260 (19)	-0.1163 (2)	0.3364 (5)	0.0555 (9)
C22	0.14987 (11)	-0.02307 (14)	0.2102 (2)	0.0214 (4)
C23	0.17449 (13)	-0.00322 (17)	0.0645 (3)	0.0285 (5)
C24	0.13755 (14)	-0.04157 (19)	-0.0852 (3)	0.0344 (5)
C25	0.07809 (14)	-0.09848 (18)	-0.0845 (3)	0.0347 (5)
C26	0.05705 (14)	-0.11353 (18)	0.0655 (3)	0.0343 (5)
H5	0.1576 (13)	-0.1717 (17)	0.441 (3)	0.023 (6)*
H4	0.2093 (14)	-0.276 (2)	0.662 (3)	0.037 (7)*
H24	0.1525 (15)	-0.028 (2)	-0.187 (4)	0.038 (7)*
H3	0.3064 (15)	-0.214 (2)	0.884 (4)	0.042 (8)*

H25	0.0550 (15)	-0.128 (2)	-0.186 (4)	0.042 (8)*
H23	0.2149 (15)	0.043 (2)	0.067 (3)	0.037 (7)*
H20A	0.4748 (15)	-0.0340 (19)	0.366 (3)	0.034 (7)*
H9	0.0375 (14)	0.0326 (19)	0.423 (3)	0.029 (6)*
H20B	0.4242 (18)	-0.013 (2)	0.194 (4)	0.060 (9)*
H2	0.3400 (15)	-0.053 (2)	0.861 (4)	0.036 (7)*
H10	-0.0068 (16)	0.148 (2)	0.583 (4)	0.045 (8)*
H26	0.0124 (16)	-0.152 (2)	0.070 (3)	0.043 (8)*
H11	0.0758 (14)	0.269 (2)	0.723 (3)	0.036 (7)*
H12	0.1939 (14)	0.272 (2)	0.692 (3)	0.037 (7)*
H18A	0.492 (2)	0.386 (3)	0.506 (5)	0.080 (12)*
H21A	0.332 (2)	-0.108 (2)	0.279 (4)	0.062 (10)*
H18B	0.495 (2)	0.317 (3)	0.373 (5)	0.079 (12)*
H21B	0.403 (2)	-0.175 (3)	0.273 (5)	0.097 (14)*
H18C	0.451 (2)	0.395 (3)	0.322 (6)	0.095 (15)*
H21C	0.385 (2)	-0.129 (3)	0.471 (5)	0.080 (12)*

Atomic displacement parameters (Å²)

	U^{11}	U^{22}	U^{33}	U^{12}	U^{13}	U^{23}
O1	0.0246 (7)	0.0169 (6)	0.0200 (6)	-0.0032 (5)	0.0065 (5)	-0.0011 (5)
O2	0.0264 (7)	0.0168 (7)	0.0225 (7)	-0.0009 (6)	0.0024 (6)	0.0027 (5)
O3	0.0292 (8)	0.0186 (7)	0.0320 (8)	-0.0061 (6)	0.0096 (6)	-0.0011 (6)
O4	0.0313 (9)	0.0360 (9)	0.0452 (10)	-0.0020 (7)	0.0176 (8)	-0.0050 (8)
O5	0.0284 (8)	0.0203 (7)	0.0424 (9)	0.0007 (6)	0.0124 (7)	-0.0039 (6)
N1	0.0246 (9)	0.0199 (8)	0.0274 (9)	-0.0048 (7)	0.0065 (7)	0.0007 (7)
N2	0.0326 (10)	0.0281 (9)	0.0279 (9)	-0.0085 (8)	0.0084 (8)	-0.0047 (7)
C1	0.0294 (11)	0.0172 (9)	0.0246 (10)	0.0018 (8)	0.0094 (8)	0.0012 (7)
C2	0.0367 (12)	0.0226 (10)	0.0264 (11)	0.0027 (9)	0.0053 (9)	0.0019 (8)
C3	0.0497 (15)	0.0225 (11)	0.0317 (12)	0.0083 (10)	0.0097 (11)	0.0078 (9)
C4	0.0482 (14)	0.0171 (10)	0.0339 (12)	0.0009 (10)	0.0120 (10)	0.0030 (9)
C5	0.0367 (12)	0.0173 (10)	0.0276 (10)	-0.0015 (8)	0.0110 (9)	-0.0017 (8)
C6	0.0266 (10)	0.0168 (9)	0.0218 (9)	0.0017 (8)	0.0093 (8)	0.0006 (7)
C7	0.0226 (10)	0.0148 (9)	0.0220 (9)	-0.0017 (7)	0.0078 (7)	0.0004 (7)
C8	0.0254 (10)	0.0138 (8)	0.0196 (9)	-0.0005 (7)	0.0067 (7)	0.0007 (7)
C9	0.0244 (10)	0.0200 (10)	0.0246 (10)	-0.0038 (8)	0.0068 (8)	0.0001 (8)
C10	0.0250 (11)	0.0265 (11)	0.0293 (11)	0.0000 (8)	0.0104 (9)	-0.0008 (8)
C11	0.0319 (12)	0.0235 (10)	0.0289 (10)	0.0021 (9)	0.0122 (9)	-0.0045 (8)
C12	0.0273 (11)	0.0185 (9)	0.0219 (9)	-0.0018 (8)	0.0046 (8)	-0.0029 (7)
C13	0.0231 (10)	0.0174 (9)	0.0190 (9)	-0.0011 (7)	0.0049 (7)	0.0015 (7)
C14	0.0251 (10)	0.0167 (9)	0.0184 (9)	0.0003 (8)	0.0040 (7)	0.0007 (7)
C15	0.0238 (10)	0.0176 (9)	0.0188 (9)	-0.0009 (7)	0.0033 (7)	-0.0001 (7)
C16	0.0245 (10)	0.0224 (10)	0.0211 (9)	-0.0012 (8)	0.0049 (8)	0.0009 (8)
C17	0.0277 (11)	0.0232 (10)	0.0239 (10)	-0.0024 (8)	0.0057 (8)	0.0003 (8)
C18	0.0354 (13)	0.0327 (13)	0.0409 (14)	-0.0113 (11)	0.0136 (11)	-0.0006 (11)
C19	0.0249 (11)	0.0271 (11)	0.0242 (10)	-0.0006 (8)	0.0052 (8)	-0.0016 (8)
C20	0.0318 (13)	0.0261 (11)	0.0424 (13)	0.0051 (9)	0.0106 (10)	-0.0080 (10)
C21	0.055 (2)	0.0274 (13)	0.093 (3)	-0.0047 (13)	0.0343 (19)	-0.0172 (15)

C22	0.0266 (10)	0.0152 (9)	0.0230 (9)	0.0007 (7)	0.0060 (8)	-0.0010 (7)
C23	0.0332 (12)	0.0287 (11)	0.0244 (10)	-0.0029 (9)	0.0078 (9)	-0.0019 (8)
C24	0.0412 (14)	0.0411 (14)	0.0219 (10)	-0.0040 (11)	0.0089 (10)	-0.0041 (9)
C25	0.0369 (13)	0.0380 (13)	0.0270 (11)	-0.0046 (10)	0.0012 (10)	-0.0094 (10)
C26	0.0344 (13)	0.0339 (12)	0.0339 (12)	-0.0100 (10)	0.0052 (10)	-0.0083 (10)

Geometric parameters (Å, °)

O1—C7	1.458 (2)	C10—C11	1.394 (3)
O1—C14	1.413 (2)	C10—H10	1.00 (3)
O2—C1	1.385 (2)	C11—C12	1.394 (3)
O2—C14	1.446 (2)	C11—H11	0.95 (3)
O3—N1	1.405 (2)	C12—C13	1.383 (3)
O3—C17	1.344 (3)	C12—H12	0.94 (3)
O4—C19	1.212 (3)	C13—C14	1.523 (3)
O5—C19	1.325 (3)	C14—C15	1.508 (3)
O5—C20	1.457 (3)	C15—C16	1.436 (3)
N1—C15	1.308 (3)	C16—C17	1.368 (3)
N2—C22	1.347 (3)	C16—C19	1.478 (3)
N2—C26	1.342 (3)	C17—C18	1.480 (3)
C1—C2	1.389 (3)	C18—H18A	0.94 (4)
C1—C6	1.399 (3)	C18—H18B	0.99 (4)
C2—C3	1.392 (3)	C18—H18C	0.86 (5)
C2—H2	0.91 (3)	C20—C21	1.489 (4)
C3—C4	1.386 (4)	C20—H20A	0.98 (3)
C3—H3	1.04 (3)	C20—H20B	1.00 (3)
C4—C5	1.397 (3)	C21—H21A	1.00 (4)
C4—H4	1.03 (3)	C21—H21B	1.08 (4)
C5—C6	1.391 (3)	C21—H21C	1.11 (4)
C5—H5	0.96 (2)	C22—C23	1.391 (3)
C6—C7	1.534 (3)	C23—C24	1.385 (3)
C7—C8	1.525 (3)	C23—H23	1.00 (3)
C7—C22	1.509 (3)	C24—C25	1.385 (4)
C8—C9	1.377 (3)	C24—H24	0.95 (3)
C8—C13	1.398 (3)	C25—C26	1.378 (3)
C9—C10	1.400 (3)	C25—H25	0.94 (3)
C9—H9	0.95 (3)	C26—H26	1.02 (3)
C14—O1—C7	103.92 (14)	O1—C14—C15	109.84 (15)
C1—O2—C14	114.43 (15)	O2—C14—C13	109.49 (15)
C17—O3—N1	109.49 (15)	O2—C14—C15	105.29 (15)
C19—O5—C20	115.89 (17)	C15—C14—C13	119.18 (16)
C15—N1—O3	105.57 (16)	N1—C15—C14	117.49 (17)
C26—N2—C22	117.14 (19)	N1—C15—C16	111.68 (18)
O2—C1—C2	116.04 (19)	C16—C15—C14	130.82 (18)
O2—C1—C6	122.66 (18)	C15—C16—C19	132.33 (19)
C2—C1—C6	121.30 (19)	C17—C16—C15	103.68 (18)
C1—C2—C3	119.2 (2)	C17—C16—C19	123.92 (19)

C1—C2—H2	122.2 (18)	O3—C17—C16	109.57 (18)
C3—C2—H2	118.5 (17)	O3—C17—C18	116.29 (19)
C2—C3—H3	120.6 (16)	C16—C17—C18	134.1 (2)
C4—C3—C2	120.4 (2)	C17—C18—H18A	115 (2)
C4—C3—H3	119.0 (16)	C17—C18—H18B	112 (2)
C3—C4—C5	119.9 (2)	C17—C18—H18C	114 (3)
C3—C4—H4	124.1 (15)	H18A—C18—H18B	98 (3)
C5—C4—H4	115.9 (15)	H18A—C18—H18C	118 (4)
C4—C5—H5	122.1 (14)	H18B—C18—H18C	97 (3)
C6—C5—C4	120.6 (2)	O4—C19—O5	124.4 (2)
C6—C5—H5	117.2 (14)	O4—C19—C16	123.2 (2)
C1—C6—C7	115.67 (17)	O5—C19—C16	112.39 (18)
C5—C6—C1	118.60 (19)	O5—C20—C21	107.0 (2)
C5—C6—C7	125.64 (19)	O5—C20—H20A	109.8 (16)
O1—C7—C6	104.89 (15)	O5—C20—H20B	110.4 (19)
O1—C7—C8	101.96 (14)	C21—C20—H20A	112.7 (16)
O1—C7—C22	108.79 (15)	C21—C20—H20B	113.4 (19)
C8—C7—C6	106.35 (15)	H20A—C20—H20B	104 (2)
C22—C7—C6	117.20 (16)	C20—C21—H21A	110 (2)
C22—C7—C8	116.05 (17)	C20—C21—H21B	109 (2)
C9—C8—C7	131.50 (18)	C20—C21—H21C	110 (2)
C9—C8—C13	121.45 (18)	H21A—C21—H21B	106 (3)
C13—C8—C7	106.83 (17)	H21A—C21—H21C	109 (3)
C8—C9—C10	118.11 (19)	H21B—C21—H21C	114 (3)
C8—C9—H9	123.0 (15)	N2—C22—C7	114.51 (17)
C10—C9—H9	118.8 (15)	N2—C22—C23	123.09 (19)
C9—C10—H10	118.4 (17)	C23—C22—C7	122.37 (18)
C11—C10—C9	120.5 (2)	C22—C23—H23	120.0 (16)
C11—C10—H10	121.1 (17)	C24—C23—C22	118.4 (2)
C10—C11—C12	120.95 (19)	C24—C23—H23	121.4 (16)
C10—C11—H11	122.8 (16)	C23—C24—H24	120.2 (17)
C12—C11—H11	116.2 (16)	C25—C24—C23	119.2 (2)
C11—C12—H12	122.3 (16)	C25—C24—H24	120.7 (17)
C13—C12—C11	118.25 (19)	C24—C25—H25	118.6 (17)
C13—C12—H12	119.5 (16)	C26—C25—C24	118.5 (2)
C8—C13—C14	106.09 (16)	C26—C25—H25	122.8 (17)
C12—C13—C8	120.70 (19)	N2—C26—C25	123.7 (2)
C12—C13—C14	132.98 (18)	N2—C26—H26	115.5 (16)
O1—C14—O2	109.19 (15)	C25—C26—H26	120.8 (16)
O1—C14—C13	103.65 (15)		
O1—C7—C8—C9	161.0 (2)	C8—C7—C22—N2	-61.9 (2)
O1—C7—C8—C13	-24.38 (19)	C8—C7—C22—C23	116.4 (2)
O1—C7—C22—N2	-176.09 (17)	C8—C9—C10—C11	-1.1 (3)
O1—C7—C22—C23	2.2 (3)	C8—C13—C14—O1	24.79 (19)
O1—C14—C15—N1	128.66 (18)	C8—C13—C14—O2	-91.61 (18)
O1—C14—C15—C16	-52.5 (3)	C8—C13—C14—C15	147.19 (17)
O2—C1—C2—C3	179.6 (2)	C9—C8—C13—C12	0.5 (3)

O2—C1—C6—C5	-179.70 (18)	C9—C8—C13—C14	175.61 (18)
O2—C1—C6—C7	-3.1 (3)	C9—C10—C11—C12	0.5 (3)
O2—C14—C15—N1	-113.89 (19)	C10—C11—C12—C13	0.6 (3)
O2—C14—C15—C16	65.0 (2)	C11—C12—C13—C8	-1.1 (3)
O3—N1—C15—C14	178.80 (15)	C11—C12—C13—C14	-174.7 (2)
O3—N1—C15—C16	-0.3 (2)	C12—C13—C14—O1	-161.0 (2)
N1—O3—C17—C16	-1.0 (2)	C12—C13—C14—O2	82.6 (3)
N1—O3—C17—C18	178.76 (19)	C12—C13—C14—C15	-38.6 (3)
N1—C15—C16—C17	-0.3 (2)	C13—C8—C9—C10	0.6 (3)
N1—C15—C16—C19	-177.3 (2)	C13—C14—C15—N1	9.4 (3)
N2—C22—C23—C24	-0.7 (3)	C13—C14—C15—C16	-171.76 (19)
C1—O2—C14—O1	-41.1 (2)	C14—O1—C7—C6	-70.50 (17)
C1—O2—C14—C13	71.8 (2)	C14—O1—C7—C8	40.23 (17)
C1—O2—C14—C15	-158.98 (16)	C14—O1—C7—C22	163.34 (15)
C1—C2—C3—C4	0.3 (4)	C14—O2—C1—C2	-174.96 (18)
C1—C6—C7—O1	35.3 (2)	C14—O2—C1—C6	4.8 (3)
C1—C6—C7—C8	-72.2 (2)	C14—C15—C16—C17	-179.22 (19)
C1—C6—C7—C22	156.07 (18)	C14—C15—C16—C19	3.8 (4)
C2—C1—C6—C5	0.0 (3)	C15—C16—C17—O3	0.8 (2)
C2—C1—C6—C7	176.65 (19)	C15—C16—C17—C18	-178.9 (3)
C2—C3—C4—C5	-0.3 (4)	C15—C16—C19—O4	171.3 (2)
C3—C4—C5—C6	0.1 (3)	C15—C16—C19—O5	-8.8 (3)
C4—C5—C6—C1	0.0 (3)	C17—O3—N1—C15	0.8 (2)
C4—C5—C6—C7	-176.3 (2)	C17—C16—C19—O4	-5.2 (3)
C5—C6—C7—O1	-148.31 (19)	C17—C16—C19—O5	174.7 (2)
C5—C6—C7—C8	104.1 (2)	C19—O5—C20—C21	-176.4 (2)
C5—C6—C7—C22	-27.6 (3)	C19—C16—C17—O3	178.15 (18)
C6—C1—C2—C3	-0.2 (3)	C19—C16—C17—C18	-1.6 (4)
C6—C7—C8—C9	-89.3 (2)	C20—O5—C19—O4	-8.2 (3)
C6—C7—C8—C13	85.24 (18)	C20—O5—C19—C16	171.90 (18)
C6—C7—C22—N2	65.2 (2)	C22—N2—C26—C25	-0.3 (4)
C6—C7—C22—C23	-116.5 (2)	C22—C7—C8—C9	43.0 (3)
C7—O1—C14—O2	76.13 (17)	C22—C7—C8—C13	-142.41 (17)
C7—O1—C14—C13	-40.49 (17)	C22—C23—C24—C25	-0.4 (4)
C7—O1—C14—C15	-168.89 (15)	C23—C24—C25—C26	1.1 (4)
C7—C8—C9—C10	174.6 (2)	C24—C25—C26—N2	-0.8 (4)
C7—C8—C13—C12	-174.74 (17)	C26—N2—C22—C7	179.4 (2)
C7—C8—C13—C14	0.4 (2)	C26—N2—C22—C23	1.1 (3)
C7—C22—C23—C24	-178.9 (2)		

Hydrogen-bond geometry (Å, °)

<i>D</i> —H... <i>A</i>	<i>D</i> —H	H... <i>A</i>	<i>D</i> ... <i>A</i>	<i>D</i> —H... <i>A</i>
C5—H5...N2	0.96 (2)	2.42 (2)	3.085 (3)	125.8 (18)
C23—H23...N1 ⁱ	1.00 (3)	2.70 (3)	3.669 (3)	163 (2)
C12—H12...O1 ⁱⁱ	0.94 (3)	2.56 (3)	3.469 (2)	162 (2)

C18—H18A···O4 ⁱⁱ	0.94 (4)	2.71 (4)	3.297 (3)	121 (3)
C18—H18B···O4	0.99 (4)	2.38 (4)	3.040 (3)	123 (3)

Symmetry codes: (i) $x, -y+1/2, z-1/2$; (ii) $x, -y+1/2, z+1/2$.